Thus T, the time to engagement, is

$$T=(GH+V_4\cdot T_2-L_2)/V_4 \tag{12}$$

The time to engagement for the attacking fighter T' must equal T to insure interdiction, where

$$T'=(R-X)/V_2 \tag{13}$$

Because of the trigonometric functions involved in the computations, the function

$$f(R')=T-T' \tag{14}$$

was formed and solved for R' by the regular falsi method[2] using a Wang 2200 to perform the repetitive calculations. Equations (4-14) were computed in turn for each pass. Since the AEW aircraft flees toward point A, the above calculations were computed within a loop of successive values of $D=D'$, formed by

$$D_i'=D-V_3\cdot(T_i-T_1) \tag{15}$$

where T_i is obtained from Eq. (12). Computations ceased when successive values of D' differed by less than 1 mile

$$|D_{i+1}'-D_i'|<=1.0 \tag{16}$$

Both Eqs. (14) and (16) are smooth valued and well formed in the region of interest: T greater than T_2. Following final solution of Eq. (14) the required radar range R was calculated by the law of cosines from triangle ABC

$$R=[D^2+AC^2-2\cdot D\cdot AC\cdot\cos(A_1)]^{1/2} \tag{17}$$

The DLI response is obtained by setting S (BARCAP station range) equal to zero, T_2 is then the DLI alert status. For the DLI response the solution to Eq. (3) is denoted by R_1(B), indicating a DLI response (R_1) to a bomber (B) attack. Similarly the solution to Eq. (17) is represented by R_1(F), indicating a DLI response to a fighter attack (F). R_2(B) and R_2(F) represent solutions to Eqs. (3) and (17), respectively, indicating a BARCAP response (R_2) to the same type of attack.

Results

In spite of the differences in geometry between this Note and that of Ref. 1, there is considerable agreement in the general trend and direction of comparable parameters. The most significant difference is in the relationship between the AEW radar range and the attacking fighter's velocity. Reference 1 indicates a concave downward function for the DLI comparable solution. This would imply that at some point the required radar range would reach a maximum and then decrease for even greater values of attacking fighter velocity. The present case (Fig. 3) indicates a monotonically increasing function for both the DLI and BARCAP response, as would be expected.

In the majority of scenarios examined by the author (Table 1), the three most significant factors requiring the largest minimum radar ranges were attacking fighter velocity, attacking bomber velocity, and standoff weapon launch range. Figures 3 and 4 depict these parameters and clearly indicate the DLI response is of major importance in minimum radar range design requirements.

References

[1] Bracken, J. and Grotte, J.H., "Required Radar Ranges for AEW Aircraft," *Journal of Aircraft*, Vol. 16, Nov. 1979, pp. 792-797.

[2] Kreyszig, E., *Advanced Engineering Mathematics*, 2nd Ed., John Wiley and Sons, New York, 1967.

AIAA 81-4193

A Geometrical Study of the Steady-State Spin for a Typical Low-Wing General Aviation Aircraft

Andrew P. Imbrie*
Princeton University, Princeton, N.J.

Introduction

In a fully evolved spin, the aircraft's center of gravity (c.g.) follows a descending helical path about the spin axis. This Note pertains to the aircraft's orientation relative to that helix, as well as the geometric and kinematic effects of the spin on the local velocity vector. Using flight test data for a low-wing general aviation aircraft,[1] this Note presents results pertaining to aircraft orientation, flow patterns, and the aerodynamic driving mechanisms in a steady-state spin.

The Kinematic Equations

It is assumed that the aircraft is in a steady-state spin with spin rate Ω, spin radius R_s, vertical velocity $w_{c.g.}$, and Euler attitude angles θ, ϕ, and $\psi-\eta$ given (Fig. 1). Coordinates of the aircraft's configuration are referred to the c.g. location along the conventional Cartesian system (x, y, and z). Referring to Fig. 1, it can be shown[2] that the orthogonal body-axis velocity components of any point p on the aircraft

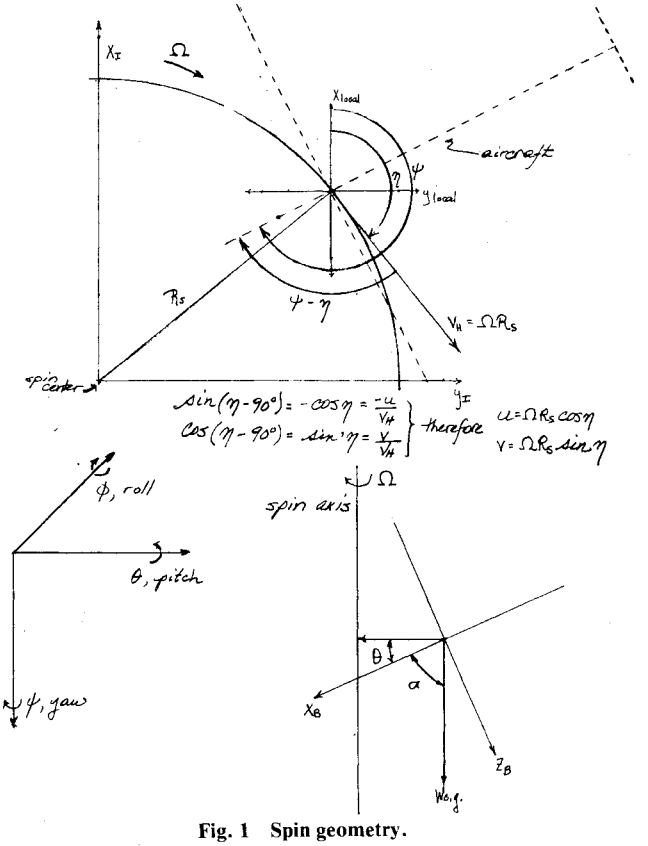

Fig. 1 Spin geometry.

Received Oct. 21, 1980; revision received Jan. 15, 1981.

*Undergraduate Student, Department of Mechanical and Aeronautical Engineering; currently Graduate Student at Stanford University.

Table 1 Spin characteristics

	Tail configuration (spin no.)				
	2	3	4a	4b	6
$\alpha_{c.g.}$, deg	55	60	51	68	62
$V_{c.g.}$, m/s	35.2	34.4	37.9	29.3	33.7
$w_{c.g.}$, m/s[a]	33.7	32.9	36.4	27.8	32.2
Ω, deg/s	155	159	157	209	167
θ, deg	−43.1	−39.0	−45.0	−27.7	−37.2
ϕ, deg	5.10	3.23	7.25	1.24	3.01
$(\psi-\eta)$, deg	116	120	107	107	121
R_s, m	3.7	3.6	3.9	2.5	3.4
p, roll rate, deg/s	106	100	111	97	101
q, pitch rate, deg/s	10	7	14	97	101
r, yaw rate, deg/s	112	124	110	185	133

[a] $w_{c.g.} = V - 1.5$ m/s.

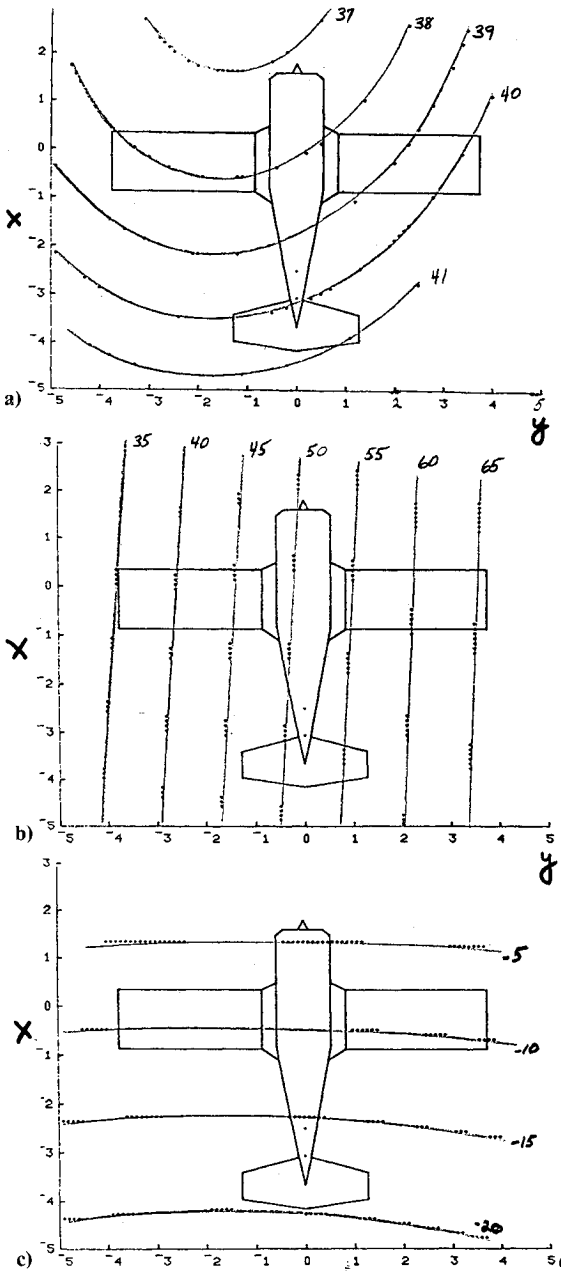

Fig. 2 Horizontal projection. a) Contours of constant V, m/s. b) Contours of constant α, deg. c) Contours of constant β, deg.

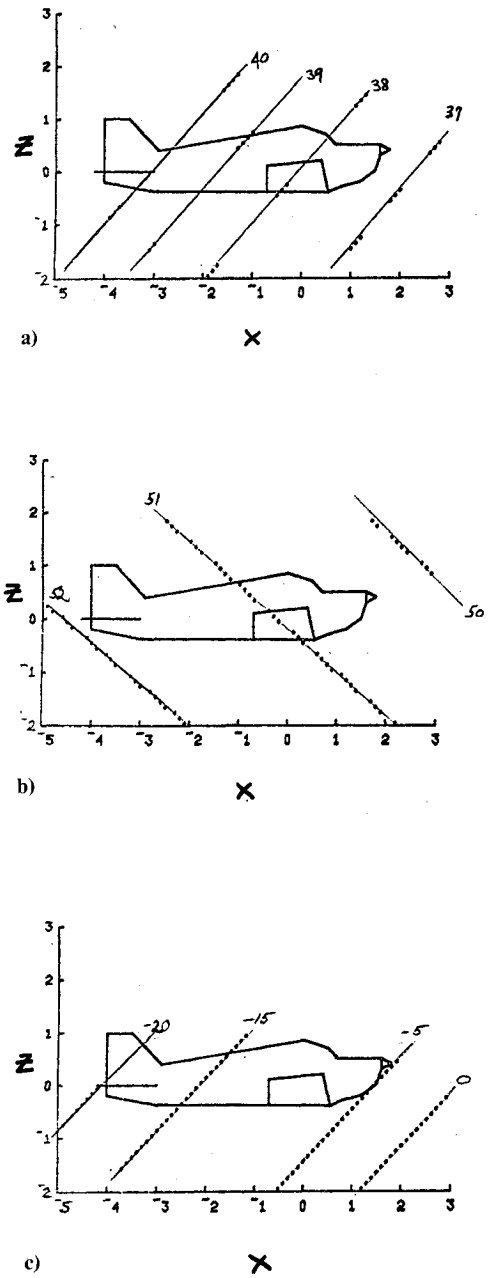

Fig. 3 Vertical projection. a) Contours of constant V, m/s. b) Contours of constant α, deg. c) Contours of constant β, deg.

are:

$$u_{p_B} = \Omega\cos\theta[R_s\cos(\psi-\eta) - y_B\cos\phi + z_B\sin(\psi-\eta)] - w_{c.g.}\sin\theta$$

$$v_{p_B} = \Omega R_s[\sin\phi\sin\theta\cos(\psi-\eta) - \cos\phi\sin(\psi-\eta)] + \Omega x_B\cos\phi\cos\theta + \Omega z_B\sin\theta + w_{c.g.}\sin\phi\cos\theta$$

$$w_{p_B} = \Omega R_s[\cos\phi\sin\theta\cos(\psi-\eta) + \sin\phi\sin(\psi-\eta)] - \Omega x_B\sin\phi\cos\theta - \Omega y_B\sin\theta + w_{c.g.}\cos\phi\cos\theta \quad (1)$$

and the corresponding polar-coordinate representations are,

$$\begin{bmatrix} V \\ \alpha \\ \beta \end{bmatrix}_p = \begin{bmatrix} (u_{p_B}^2 + v_{p_B}^2 + w_{p_B}^2)^{1/2} \\ \tan^{-1}(w_{p_B}/u_{p_B}) \\ \sin^{-1}(v_{p_B}/V) \end{bmatrix} \quad (2)$$

Aircraft Orientation

Data for five spin modes resulting from various tail modifications are given in Ref. 3. Flight variables referenced to the c.g. are presented in Table 1. The variables θ and ϕ are found from:

$$\theta = \sin^{-1}(-p/\Omega) \qquad \phi = \tan^{-1}(q/r) \quad (3)$$

R_s is found by: $R_s = \sqrt{V^2 - w_{c.g.}^2}\,(1/\Omega)$. V and $\alpha_{c.g.}$ are given, and $\psi-\eta$ is found numerically. These values also are presented in Table 1.

Referring to Table 1, it is found that $\psi-\eta$ is greater than 90 deg for all spin modes: i.e., the aircraft's nose not only points toward the center of the spin, but lags behind it even though $\beta_{c.g.}$ is considerably smaller than $\psi-\eta$. The velocity in the horizontal direction v_H (Fig. 1) is much less than the vertical velocity $w_{c.g.}$; therefore, the primary motion is downward, not circular, and the results are consistent. (Similar results are presented for high-performance aircraft in Ref. 4.) The spin radii R_s is within the wing span, as might be anticipated.[5]

Geometric Description of the Flow

Given the data of Table 1 and the equations derived above, it is possible to plot contours of constant V, α, and β over the aircraft, such as those shown in Figs. 2 and 3. It should be realized when viewing these figures that the airplane is pitched, rolled, and yawed with respect to the inertial frame; consequently, the distributions of V, α, and β are somewhat complex.

The location of the center of the spin relative to the aircraft is inferred from the velocity magnitude distribution (Fig. 2a): the nonzero roll angle causes the deviation of the velocity curves from perfect circles. The pitch angle has a major effect on distributions in the aircraft's vertical plane (Fig. 3). The direction of the spin (Fig. 2a) is clockwise about the spin axis. The velocity ranges from about 28 m/s at the nose in spin 4b to about 42 m/s at the tail in spin 4a.

Lines of constant α are almost parallel to the fuselage and range in value from about 35 deg at the left wingtip in spin 4b to greater than 90 deg at the right wingtip in spin 4a. The very large variation of α over the wing span causes a large variation in lift and, therefore, in induced drag: the drag on the right (retreating) wing is much greater than on the left (advancing) wing. There is little variation of α in the vertical plane (Fig. 2b).

Lines of constant β are nearly perpendicular to the fuselage (Fig. 2c), and range from about -35 deg at the tail in spin 4b to about -5 deg at the nose in all the spins. The flow over the vertical tail tends to oppose the spin; however, at the very high angles of attack involved, the tail's restoring moment could be reduced by interference in the flow from the wings and fuselage. There is a large β variation in the vertical plane (Fig. 3c).

Driving Mechanism

A rudimentary application of strip theory[1] suggests that the driving mechanism for the spin is the differential induced drag on the aircraft's wings. For the analysis, it was assumed that the flow was two-dimensional and that the only significant contributions to the forces and moments came from the wings, horizontal tail, and vertical tail.

As mentioned above, the retreating wing is at a higher angle of attack and therefore has a higher induced drag than the advancing wing. This is what drives the spin. Opposing the spin is the side force (acting through a moment arm about the center of gravity) on the vertical tail. This result is consistent with the qualitative guidance provided by Ref. 5.

Conclusions

This Note has presented a preliminary analysis of the geometric properties of a fully evolved spin and their effects on the flowfield about a general aviation aircraft. The results could form the basis for an analytical study of the forces and moments acting on a spinning aircraft, and they provide insights regarding the underlying causes of the spin.

Acknowledgments

This research was funded in part by The Schultz Foundation of Clifton, N.J. The author wishes to thank Profs. R. Stengel and D.C. Hazen for their assistance in the preparation of this Note.

References

[1] Imbrie, A.P., "A Geometrical Study of the Steady State Spin for a Typical Low Wing General Aviation Aircraft," BSE Thesis, Princeton University, Princeton, N.J., 1980.

[2] Kaplan, M.H., *Modern Spacecraft Dynamics and Control,* John Wiley & Sons, New York, 1976, p. 15.

[3] Patton, J.M., Stough, H.P., and Dicarlo, D.J., "Spin Flight Research Summary," SAE Paper 790565, April 1979.

[4] Adams, W.M., "Analytic Prediction of Airplane Equilibrium Spin Characteristics," NASA TND-6926, Nov. 1972.

[5] Gates, S.B. and Bryant, L.W., "The Spinning of Aeroplanes," Aeronautical Research Committee, R & M 1001, Oct. 1926.

Errata

Reply by Author to P. R. Payne

J. A. C. Kentfield*
University of Calgary, Calgary, Alberta, Canada
[J. Aircraft, **17**, 544 (1980)]

THE references cited in the first paragraph are incorrect. Reference 6 should be Ref. 7 and Ref. 7 should be Ref. 8.

Received Sept 29, 1980.

*Professor, Dept. of Mechanical Engineering. Member AIAA.